

LOW-VOLTAGE BANDGAP REFERENCE DESIGN  
UTILIZING SCHOTTKY DIODES

by

David L. Butler

A project

submitted in partial fulfillment

of the requirements for the degree of

Master of Science in Engineering, Electrical Engineering

Boise State University

March, 2005

© 2005

David L. Butler

ALL RIGHTS RESERVED



## ABSTRACT

As semiconductor device geometries continue to shrink, the corresponding voltage applied across the processed devices must also be reduced. Therefore reference voltages used in integrated circuits will need to have lower values. A typical bandgap reference (BGR) voltage generator uses PN junction diodes or PNP BJT's to bias the reference. The forward bias voltage of these devices is typically 0.7 volts, and has a limiting effect on circuit voltage and how low a reference voltage can be generated. Schottky, or metal-semiconductor (MS), diodes have a lower forward bias voltage, typically of about 0.3 volts. The implementation of Schottky metal-semiconductor diodes in place of PN diodes in the design of a BGR, should allow for lower reference voltage generation.

In this project, a BGR was designed and fabricated using a 0.5 $\mu$ m process. Schottky diodes were also fabricated on the chip. After fabrication, the diodes were experimentally characterized and modeled in SPICE. The SPICE model was used to design a functional BGR. The BGR circuit with Schottky diodes was then tested and validated as functional.

Measured results indicate a MS diode threshold voltage thermal characteristic of -0.56mV/ $^{\circ}$ C. With several parts evaluated, the BGR circuits produced a reference voltage with a voltage gradient of a low of 7mV/V, to a high of 24mV/V, across a one volt VDD sweep. Temperature coefficients ranging from -107ppm/ $^{\circ}$ C to 500ppm/ $^{\circ}$ C were measured.

## TABLE OF CONTENTS

ABSTRACT.....	iv
LIST OF FIGURES.....	vii
CHAPTER ONE: INTRODUCTION.....	1
Introduction.....	1
CHAPTER TWO: SCHOTTKY DIODE.....	3
Schottky Diode Operation.....	3
Schottky Diode Fabrication Overview.....	4
CHAPTER THREE: THEORY AND BGR DESIGN.....	5
Circuit Design.....	5
Layout.....	7
Fabrication Process.....	10
Schottky Diode Fabrication.....	11
Fabrication Results.....	12
CHAPTER FOUR: MEASURED RESULTS.....	16
Diode Characterization.....	16
BGR Simulation.....	19
BGR Circuit Measurements.....	23
Diode Process Variation Evaluation.....	28

CHAPTER FIVE: CONCLUSION.....	31
Conclusion.....	31
Future Work.....	31
REFERENCES.....	35
APPENDIX A: Final Design Netlist.....	36
APPENDIX B: Future Design Netlist.....	40

## LIST OF FIGURES

Figure 2.1: MS Junction Energy Bandgap.....	3
Figure 2.2: Schottky Diode Cross Section.....	4
Figure 3.1: Bandgap Reference Circuit Design.....	5
Figure 3.2: Chip Layout.....	8
Figure 3.3: Schottky Diode Layout.....	9
Figure 3.4: BGR Circuit Layout.....	10
Figure 3.5: Full Chip Photo.....	13
Figure 3.6: Schottky Diode Photo.....	14
Figure 3.7: BGR Circuit Photo.....	15
Figure 4.1: Schottky Diode I-V vs. Temperature.....	17
Figure 4.2: MS Diode I-V Curve Model.....	18
Figure 4.3: BGR Simulation Results.....	22
Figure 4.4: Final BGR Design.....	23
Figure 4.5: Measured Reference Voltage.....	24
Figure 4.6: Pre-Post Trim Measurements.....	25
Figure 4.7: BGR Temperature Behavior.....	26
Figure 4.8: BGR Thermal Comparison.....	27
Figure 4.9: MS Diode I-V Distribution.....	29

Figure 4.10: MS Diode $V_t$ Distribution.....	30
Figure 5.1: Future BGR Design.....	32
Figure 5.2: Future BGR Simulation.....	33



## CHAPTER ONE: INTRODUCTION

### Introduction

As semiconductor device geometries continue to shrink, the corresponding voltage applied across the processed devices must also be reduced. Therefore reference voltages used in integrated circuits will need to be reduced as well. A typical bandgap reference (BGR) voltage generator uses PN junction diodes or PNP BJT's to bias the reference. The forward bias voltage of these devices is typically 0.7 volts, and has a limiting effect on how low a reference voltage can be generated, as well as how low a system voltage can be applied. Schottky, or metal-semiconductor (MS), diodes have a lower forward bias voltage, typically of about 0.3 volts. The implementation of Schottky metal-semiconductor diodes in place of PN diodes in the design of the BGR, should allow for lower reference voltage generation. This project consists of the design and simulation of a BGR utilizing MS diodes, followed by fabrication and validation of the design.

The bandgap reference voltage generator is designed to provide a stable reference voltage across the device operating temperature and voltage. The BGR should also be functionally stable regardless of typical process variations. This circuit is a low voltage reference design for short channel processes. The design uses a known BGR circuit, but replaces the PN junction diodes, with MS diodes [1].

The BGR design validation process will involve several steps. First is to simulate the design operability of the BGR after replacement of the PN diodes in the circuit with the

MS diodes. An approximated Schottky diode model will be used to estimate the actual operation. The modeled circuit will then be laid out and fabricated in a short channel CMOS process. The actual diodes and resistors will not be connected, but bonded in after fabrication to allow for post fabrication circuit adjustments. Once the actual MS diodes have been fabricated, the operational characteristics will be recorded and the simulation SPICE model will be updated accordingly. With this more accurate diode model, the BRG circuit design will then be further simulated to achieve an optimized reference. Then the final circuit will be built and characterized. Design validation will involve showing acceptable BGR operation, measured across nominal voltage, temperature and process variations.

## CHAPTER TWO: SCHOTTKY DIODE

### Schottky Diode Operation

The Schottky, or metal-semiconductor (MS), diode is formed by the contact of a metal to a semiconductor. The function of the Schottky diode operation differs from the PN junction diode (most notably) in that it typically has a lower forward bias threshold voltage. In this application, the lower threshold voltage is the advantageous feature.

When metal is contacted to a low dose N type semiconductor, electrons in the semiconductor move into the metal, leaving behind holes and forming a potential charge between the semiconductor and the metal [2]. This forms the rectifying contact of the MS diode. An example of the resulting (a) pre and (b) post metal semiconductor contact energy bandgap is shown in Figure 2.1 [3].

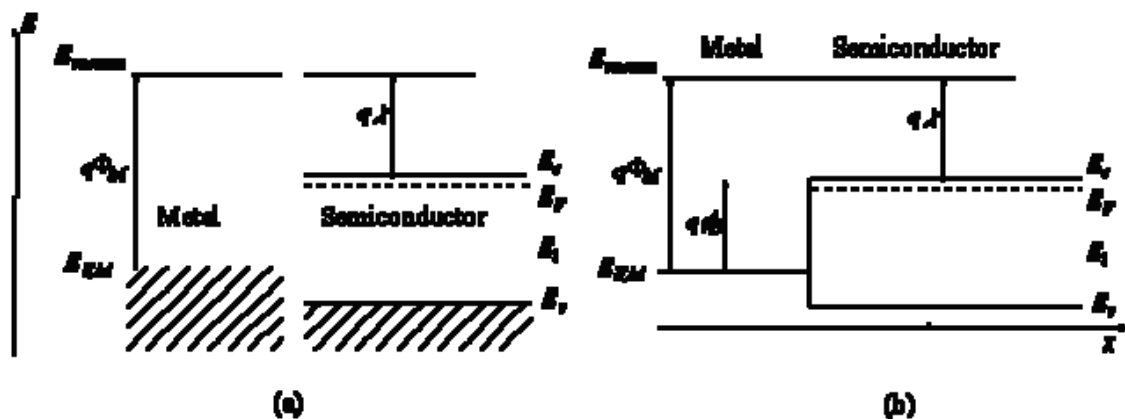
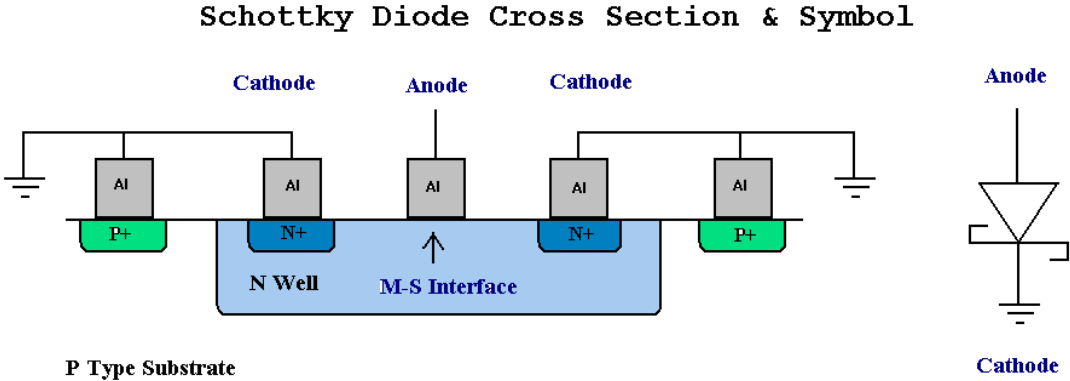


Figure 2.1 MS Junction Energy Bandgap

Although this explanation of the MS diode operation is perhaps oversimplified for the purpose of developing a basic understanding of diode operation, there are many other factors at work [4].

### Schottky Diode Fabrication Overview

In this fabrication, the MS diode rectifying contact will be formed by deposition of a metal (TiN/AlCu/TiN) on an N-well silicon. The ohmic contact will be made by contacting the same N-well to metal but through an N+ active area. The ohmic contact will then be routed to a ground plane. The cross section and accompanying schematic are shown in Figure 2.2.



**Figure 2.2 Schottky Diode Cross Section**

The MS (rectifying) interface is located under the anode contact to the well. The ohmic contact is formed in the N+ area. Here there are too many donor atoms to allow for the formation of a depletion region. The cathode is connected to ground since the operation of this circuit requires only forward bias operation.

## CHAPTER THREE: THEORY AND BGR DESIGN

### Circuit Design

The bandgap reference (BGR) voltage generator is designed to provide a stable reference voltage across operating voltage and temperatures, while exhibiting minimum process variation effects. This design uses a known BGR circuit, but replaces the PN junction diodes, with MS diodes [1]. Since MS diodes have a lower forward bias voltage (approximately 0.3V) than PN diodes (approximately 0.7V), this should allow for a lower reference voltage generation. It will also allow the circuit to operate in a lower voltage system. The general circuit design is shown here in Figure 3.1.

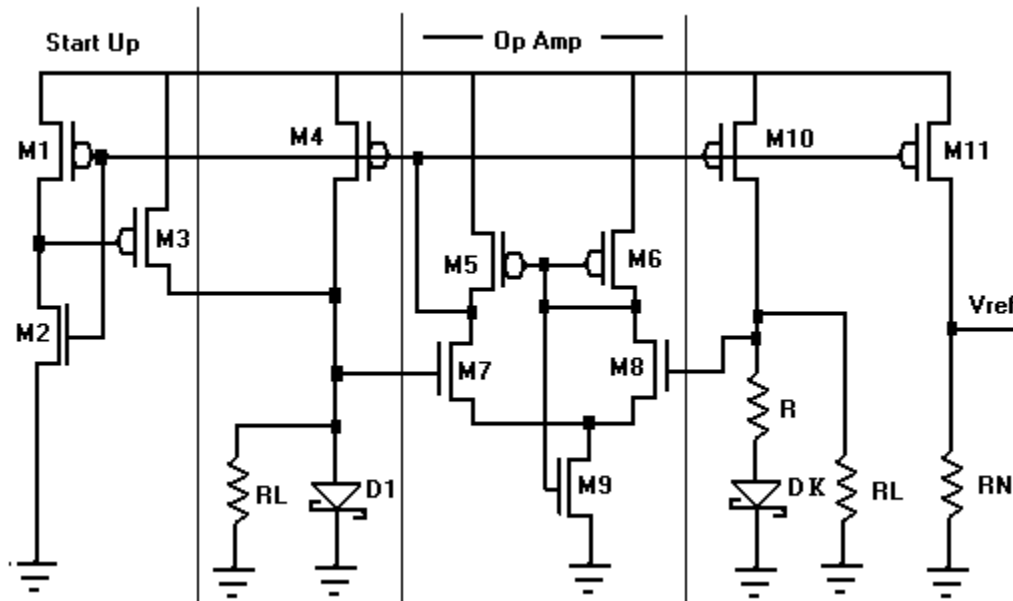


Figure 3.1 Bandgap Reference Circuit Design

The bandgap reference generates a stable voltage over temperature ranges utilizing devices with properties that are proportional to absolute temperature (PTAT) and complementary to absolute temperature (CTAT). PTAT properties are those that exhibit increased current flow at increased temperature. CTAT are those that are complementary. The circuits are used to complement each other thus providing for a more stable temperature performance than is possible with each alone [1].

The portions of the circuit that operate proportional to absolute temperature are the diodes D1 and diode DK along with its series resistor R. This is because the diode voltage decreases with increasing temperature, allowing increased current flow through the diode at higher temperatures. The PTAT current equation is given by Equation 3.1.

$$I_{PTAT} = \frac{nV_T * \ln K}{R} \quad \text{EQ 3.1}$$

The portions of the circuit that operates complementary to absolute temperature are the resistors which are labeled as R\*L. This is because the resistance increases with increasing temperature, causing a reduction in the current flowing through the resistors at higher temperatures.

$$I_{CTAT} = \frac{V_{D1}}{R * L} \quad \text{EQ 3.2}$$

To some extent, this counters the increased current through the diodes and helps stabilize the current flow through the reference making a more thermally stable reference voltage. The overall temperature behavior of the BGR is modeled by the following equation:

$$\frac{\partial V_{REF}}{\partial T} = n * N * \ln K * \frac{\partial V_T}{\partial T} + \frac{N}{L} * \frac{\partial V_{D1}}{\partial T} \quad \text{EQ 3.3}$$

Since the diodes in the circuit would have to be fabricated and characterized before the circuit resistor values could be determined, the resistors would not be fabricated in the layout, but would be applied externally after fabrication. The rest of the circuit (the MOSFET portion) was designed based on SPICE simulation models, based on estimates of the MS diodes anticipated operation [5]. The circuit was then ready for layout.

## **LAYOUT**

The actual physical implementation of the design was laid out using the LASI layout program [6]. The layout of the chips circuits were completed as shown in Figure 3.2. The layout included four BGR circuits and two diode designs. Although the first design is the one of focus, the other designs were included for redundancy in the event the first circuit and diode designs did not function as expected. Since these other circuits and diodes were not used in this project, they will not be mentioned further.

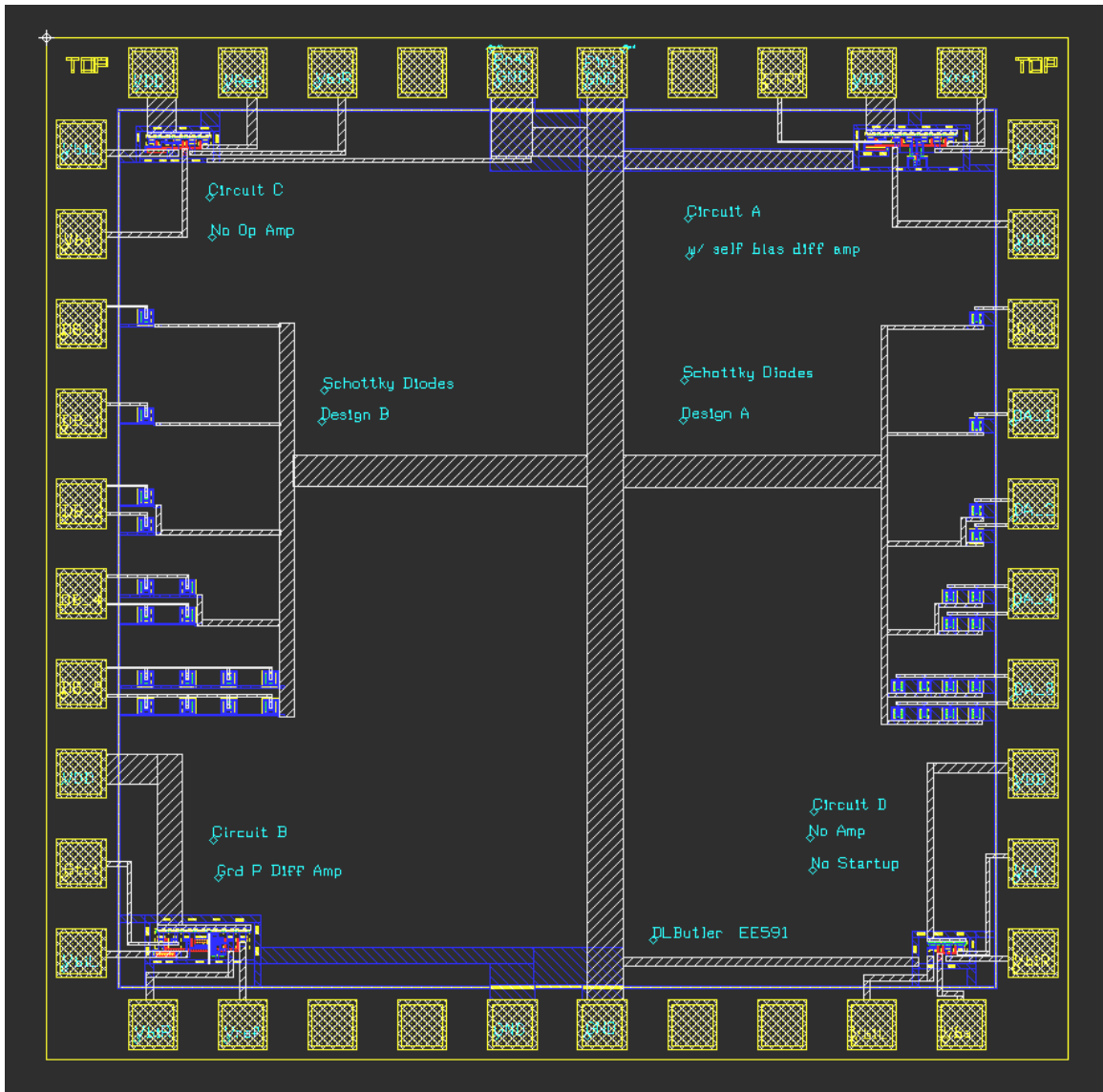


**Figure 3.2 Chip Layout**

The layout of the tested BGR circuit is the one in the top right corner of the layout. The MS diodes that were used are on the right side. These were laid out as single diodes of the same design. But to allow for larger multiple diodes for DK, (larger K) single diodes were also grouped in clusters of 2, 4 and 8. These are referred to as x1, x2, x4, and x8 respectively. The diode layout in detail is shown in Figure 3.3.



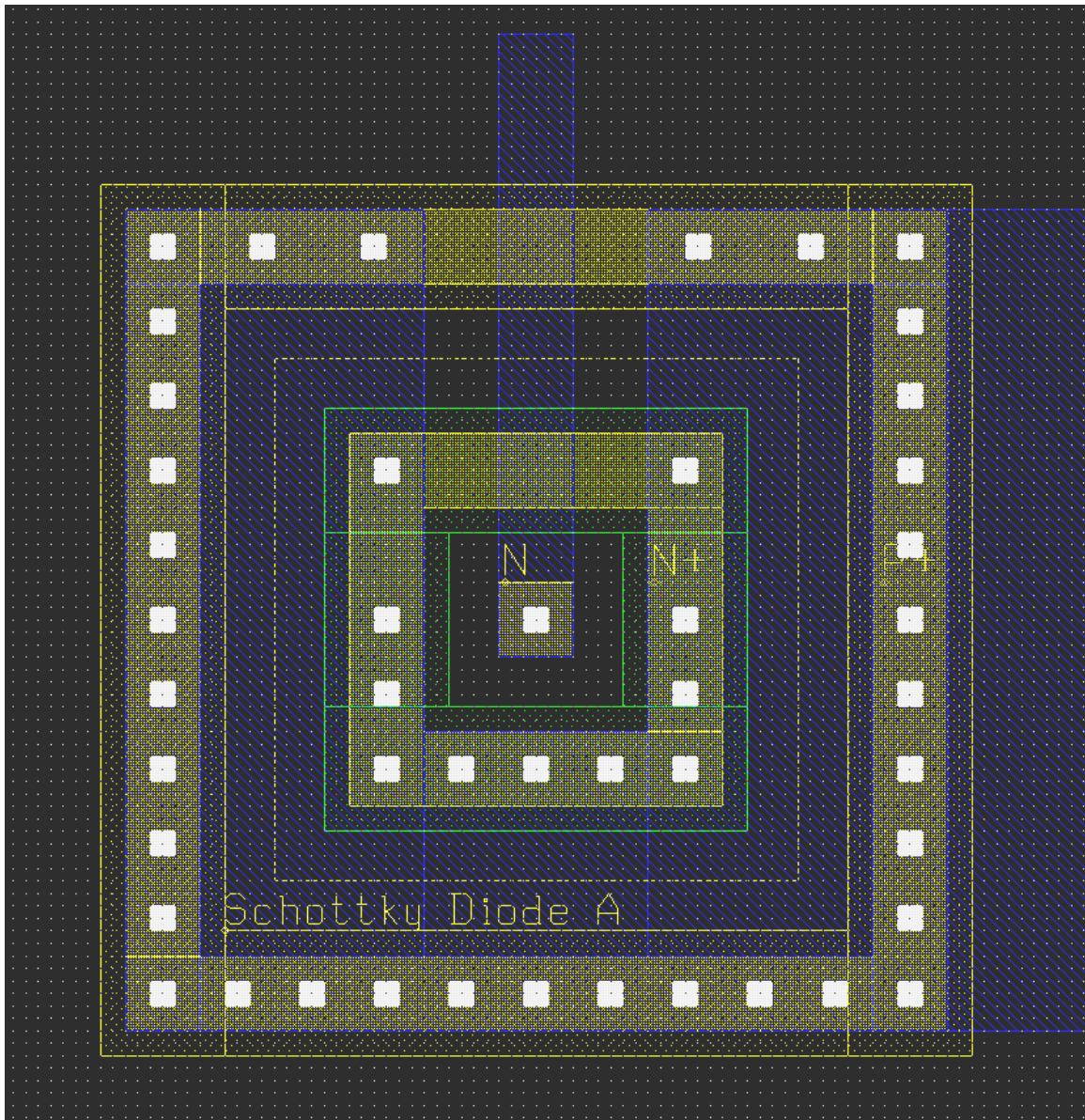


**Figure 3.3 Schottky Diode Layout**

A close-up of the layout of the circuit that was tested can be seen in Figure 3.4. The outputs are routed to bond pads as to allow for external manipulation of the circuit.

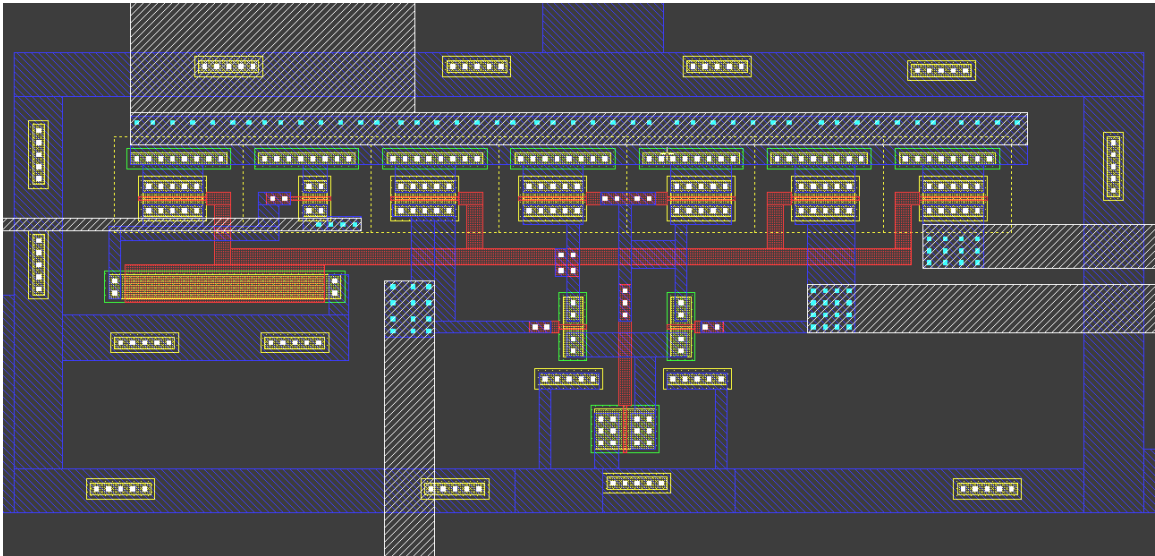


**Figure 3.4 BGR Circuit Layout**

### **Fabrication Process**

The microchip was fabricated through a MOSIS fabrication organization [7]. The specific fabrication facility was American Microsystems Inc. (AMI) [8]. The AMI foundry produced the chip using their  $0.5\mu\text{m}$  process designated AMI\_C5F by MOSIS. The Technology code is SCN3ME\_SUBM. This defines the process as scalable CMOS N-well with 3 metal layers and electrode (poly2) availability for capacitors. The SUBM designation indicates the process is submicron. The process has a P-type substrate and uses aluminum (TiN/AlCu/TiN) at metal levels.

The AMI process uses a scalable lambda design rule with minimum features of 2 lambda. This allows the same design features to be used across several different feature size processes. Each lambda actual feature size is  $0.3\mu\text{m}$  for this process series.

Therefore the minimum feature on this process run is  $0.6\mu\text{m}$ , with the exception of contacts and vias which are  $0.5\mu\text{m}$ .

There are 17 fabrication mask layers available. These layers are the N-well, active, poly, N+, P+, poly2, high resistance implant, four contact layers, Metal1, via1, Metal2, via2, Metal3 and glass. Minimum design rules for feature size, spacing and overlaps vary by specific levels.

The overall chips size was  $1.5\text{mm} \times 1.5\text{mm}$ . The 40 bond pads are  $72\mu\text{m} \times 72\mu\text{m}$ , with a passivation opening of  $60\mu\text{m} \times 60\mu\text{m}$ . This is the minimum opening size for bonding on this process.

The specific fabrication run that the chip was produced on is run number T4BP. The die itself is "AE", and five parts were produced. The run started on 11/29/04 and actually entered fabrication on 12/06/04. After the parts completed fabrication, they were then sent to a packager to be packaged in a 40pin DIP package. The packaged parts were received back on 2/4/05.

### **Schottky Diode Fabrication**

The AMI C5N process allows for the fabrication of the Metal Semiconductor diode. Also known as a Schottky diode, the MS diode is (in this process) formed by first creating an N-well in the P-type substrate. Then an opening to the silicon (through the glass) of the N-well is created by the selection of the active layer. Unlike the more common use of the active layer as an ohmic contact, no N+ implant is selected, but rather

a contact is selected and the metal is deposited on the N-well. This metal to low implant N-well semiconductor forms a metal semiconductor rectifying diode.

The cathode of the diode is connected using a common ohmic contact. It is formed in the same N-well by means of a contact. But in this case the N+ layer is selecting facilitating a high N+ type implant to the active opening, which allows for a reduced contact resistance. For this project, the ohmic contact is grounded. This ensures the entire N-well is also tied to ground. Contacts are also applied around the N-well in the substrate. The contacts are applied through an active and P+ layer to ensure the substrate is also tied to ground. This reduces substrate injection which could cause voltage and current fluctuations in the substrate that could alter the bias (possibly a forward biasing) of the diode, or possibly affecting other circuits.

The MS diode has an estimated area (metal to semiconductor contact area) of 0.25 square micrometers. This is since the contact size of this process is  $0.5\mu\text{m}$ , thus  $(0.5\mu\text{m}) \cdot (0.5\mu\text{m}) = 0.25\mu\text{m}^2$ .

### **Fabrication Results**

A photo of the fabricated and packaged chip is shown in Figure 3.5. Most visible are the large ground busses that cross the die. Since there were few circuits fabricated, there was ample room for significant and redundant grounding. Although all circuits and the substrate shared the ground busses, individual circuits had their own power rails. This would prevent a defect in one circuit from affecting other circuits on the chip.

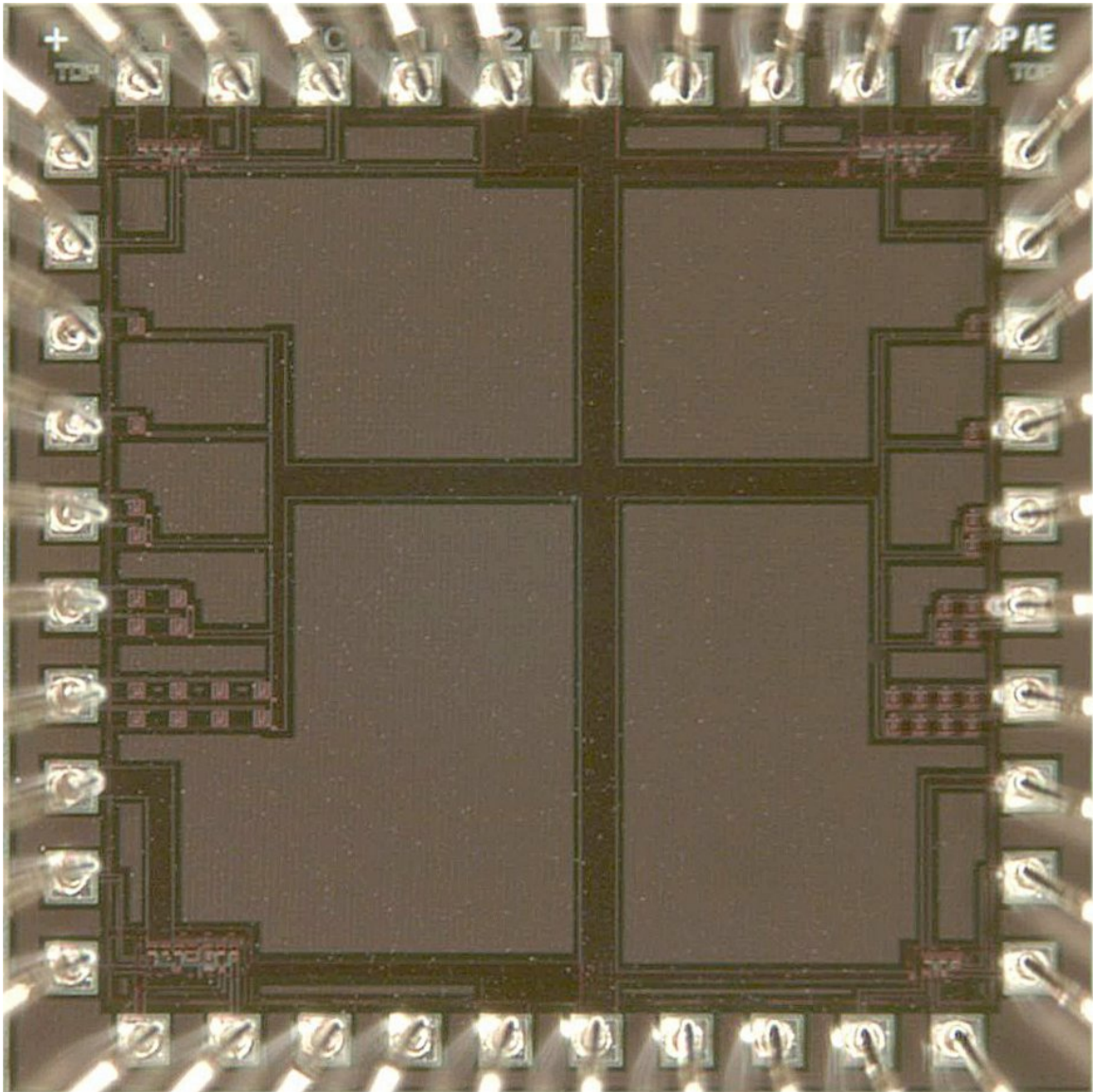


**Figure 3.5 Full Chip Photo**

Although the individual circuits are not visible at such low magnification, a close up of the MS diode and BGR circuit are included in Figure 3.6 and Figure 3.7 respectively.



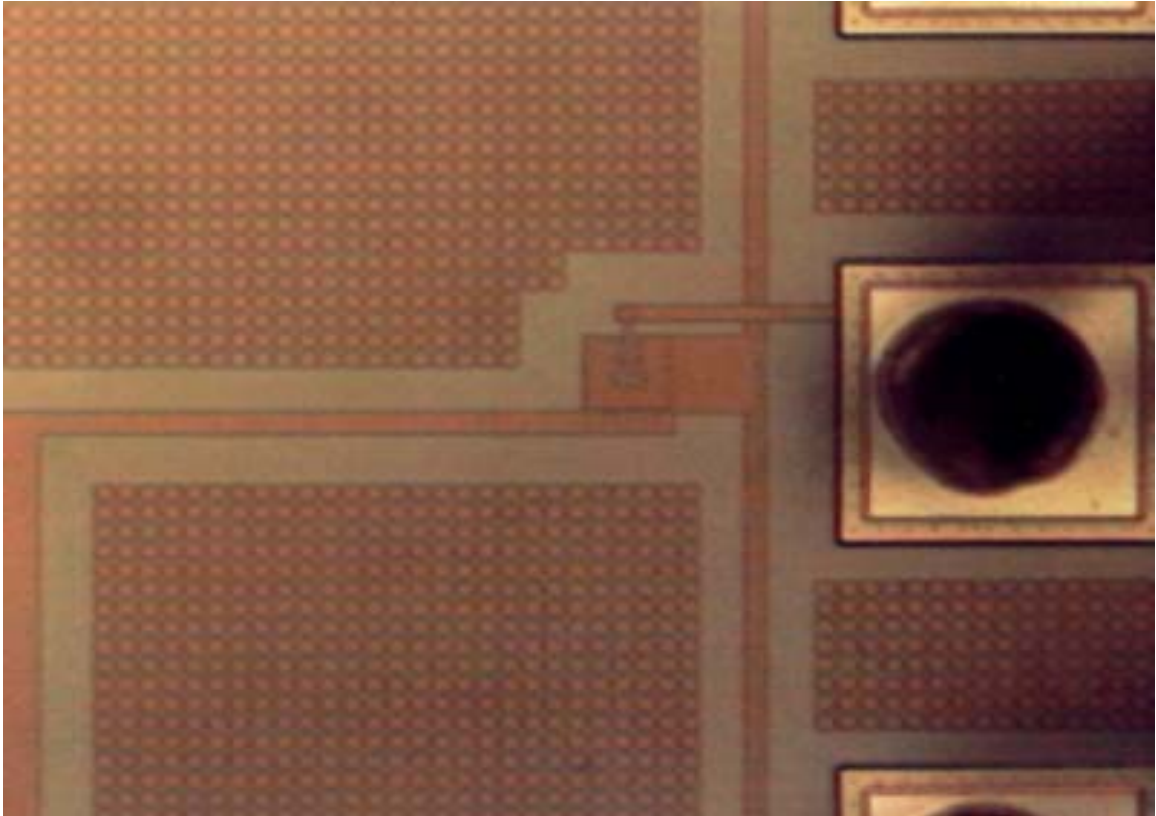


**Figure 3.6 Schottky Diode Photo**

Metal fill can be seen around the diode structure; these are the small evenly placed squares. They are used by the fabrication facility to ensure uniformity (level planarity) during processing.

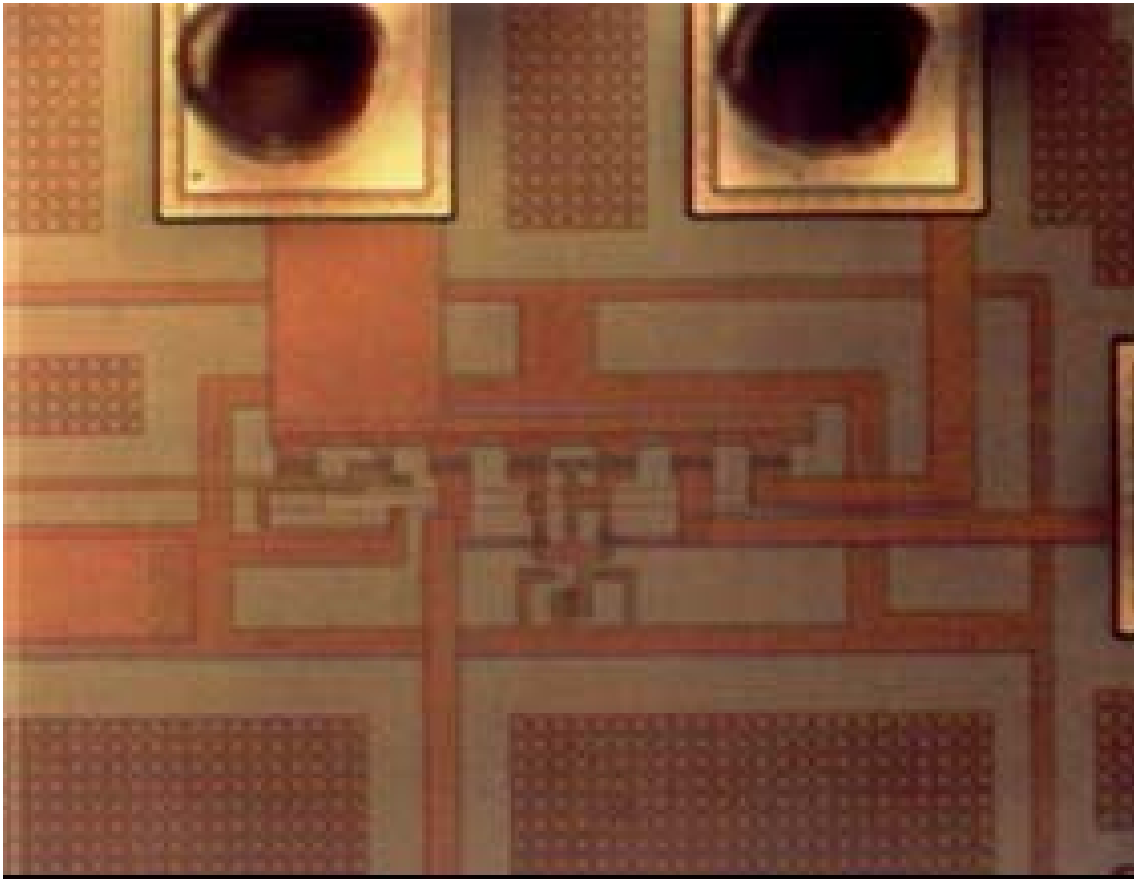


**Figure 3.7 BGR Circuit Photo**

This is the circuit as it was evaluated. Visible are the metal layers and several bond pads, through which the circuit is accessed.

## CHAPTER FOUR: MEASURED RESULTS

### Diode Characterization

The Schottky diodes in the circuit were characterized to determine their actual operational characteristics, in order to form a more precise diode model in SPICE. This model would then be used in simulating the BGR circuit operation. Therefore a close approximation of the MS diode model, and not an exact fit, was needed to get the BGR to function. The diode current equation (ignoring series and shunt resistances) is given below in Equation 4.1 [9]. Since the operation of this circuit does not involve reverse bias components, these were not characterized.

$$I_D = I_s \left( \exp \left\{ \frac{qV_D}{nkT} \right\} - 1 \right) \quad \text{EQ 4.1}$$

The tests run were voltage sweeps. These were run across operating voltage and temperature, in order to determine current-voltage (I-V) curves over input voltage range and temperature. This first test was run from 0V volt to 1.0V, and at 0°C, 25°C and 70°C. Since the area of operation that is of interest for the BGR is below 0.6V, all future measurements were from 0V to 0.6V. Figure 4.1 shows the resulting measured I-V characteristics of a single diode.



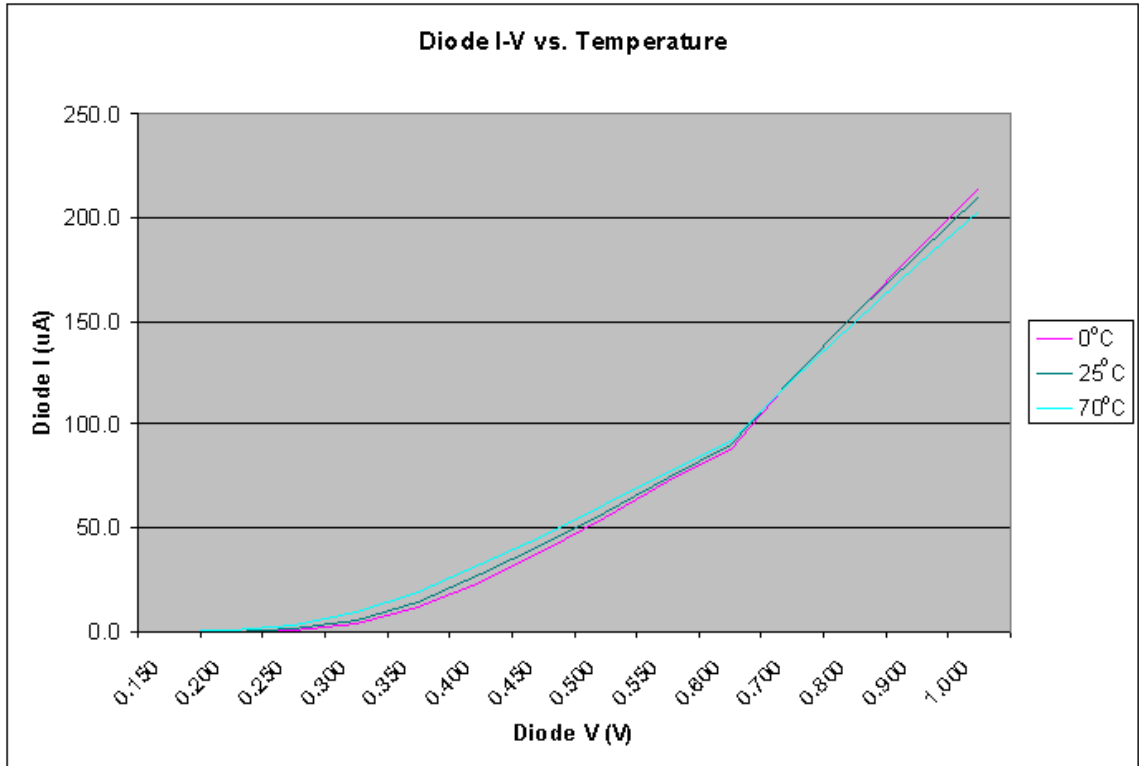


**Figure 4.1 Schottky Diode I-V vs. Temperature**

Note that there is a thermal crossover at about 0.75V, this is due to the internal resistance in the diode, which allows the IR component of the current equation to dominate at higher voltages. That is why low voltage operation is preferred.

This measured data was used to determine a temperature coefficient. It is evident that the diode change in voltage with temperature is CTAT, as determined by equation 4.2.

$$\frac{\partial V_D}{\partial T} = \frac{V @ T_{\max} - V @ T_{\min}}{T_{\max} - T_{\min}} \quad \text{EQ 4.2}$$

The measured averaged results on two diodes indicated that the value is  $-0.56 \text{ mV}/^\circ\text{C}$ .

This was determined by using a set current and measuring the voltage at  $0^\circ\text{C}$  and  $70^\circ\text{C}$ .

In this case three currents were used ( $3\mu\text{A}$ ,  $5\mu\text{A}$  and  $10\mu\text{A}$ ) and the results were

averaged. This brings up the point, that although most devices functioned similarly, there was significant current and thermal variation between diodes.

Based on measured results, the MS diode resistance was determined to be approximately  $3.2\text{k}\Omega$ . This was determined by the slope of the I-V curve from  $0.4\text{V}$  to  $0.6\text{V}$ , since the series resistance is one divided by the slope of the I-V curve. The ideality factor ( $n$ ) and saturation current ( $I_s$ ) were estimated by applying values to the SPICE simulation, and modeling it to the actual measured curve. Using this method,  $n$  was determined to be approx  $0.41$  and  $I_s$  was set to  $4 * 10^{-18}\text{A}$ . The resulting simulation is shown in Figure 4.2, overlaid with the average I-V curve of several measured diodes.

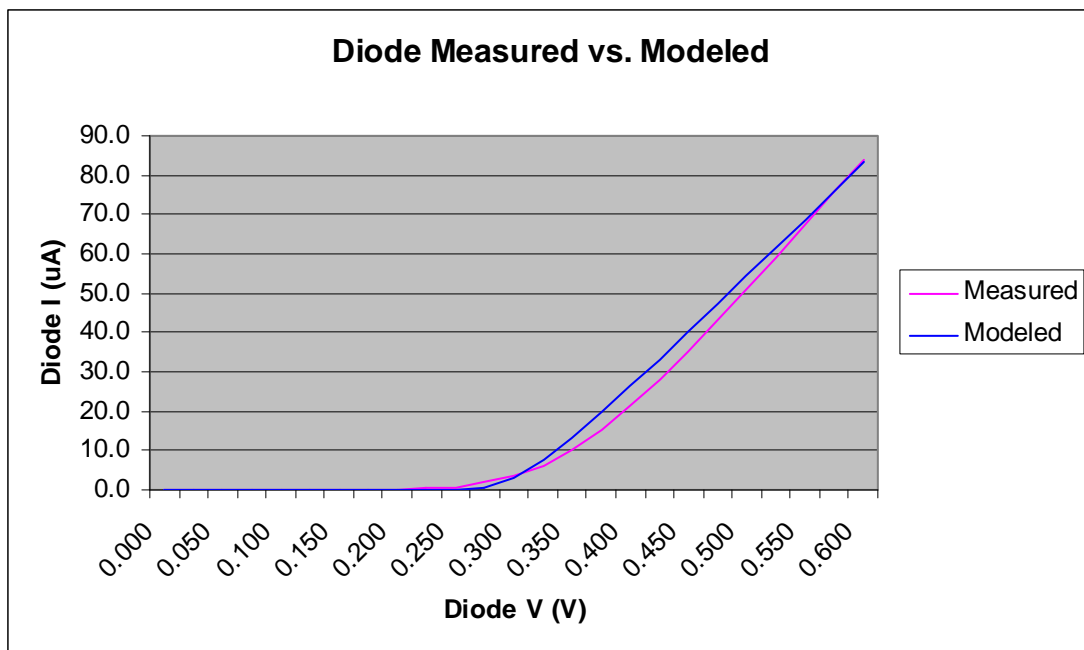


**Figure 4.2 MS Diode I-V Curve Model**

### BGR Simulation

With this close approximation of the diode behavior modeled in SPICE, the BGR circuit was then designed. The values of the resistor R, and ratios N and L, were calculated as follows and used in the model, with the R\*N (Rref) value being trimmed as needed for the best performance. A value of 8 was used for K, as the largest diode structure fabricated had eight individual diodes.

As noted earlier, the BGR thermal behavior is shown in Equation 4.3 [1].

$$\frac{\partial V_{REF}}{\partial T} = n * N * \ln K * \frac{\partial V_T}{\partial T} + \frac{N}{L} * \frac{\partial V_{D1}}{\partial T} \quad \text{EQ 4.3}$$

With the diode measurements taken relative to temperature (as previously noted), the diode thermal derivatives was determined to be:

$$\frac{\partial V_{D1}}{\partial T} = -0.56\text{mV}/^\circ\text{C}$$

Since the design involved unknown resistor values, external 1/8W carbon film resistors were implemented. The thermal effect was minimal because of the ratios used in the design, and is expected to be minimal on actual fabricated resistors.

$$\frac{\partial V_T}{\partial T} = 0.085\text{mV}/^\circ\text{C}$$

With this information, and setting the temperature coefficient (TC) to zero (desired), the following were solved for. First L is determined through the following equation:

$$L = \frac{-\frac{\partial V_{D1}}{\partial T}}{n * \ln K * \frac{\partial V_T}{\partial T}} \quad \text{EQ 4.4}$$

$$L = \frac{0.56}{0.41 * 2.08 * 0.085} = 7.7$$

Next N was solved as is indicated in the following equation:

$$N = \frac{V_{REF}}{nV_T * \ln K + \frac{V_{D1}}{L}} \quad \text{EQ 4.5}$$

$$N = \frac{0.4V}{0.41 * 0.026 * 2.08 + \frac{0.3V}{7.7}} = 6.6$$

With the diode current estimated at 1μA, R was solved for from the following equation:

$$R = \frac{n * V_T * \ln K}{I} \quad \text{EQ 4.6}$$

$$R = \frac{0.41 * 0.026 * 2.08}{1 \times 10^{-6}} = 22k\Omega$$

With these values, resistors were set as follows:

$$R * L = 22k\Omega * 7.7 = 172k\Omega$$

$$R * N = 22k\Omega * 6.6 = 145k\Omega$$

Since the goal was to develop a low voltage reference, a voltage of 0.4 volts was selected as a target. This is an arbitrary point, but it is within the low voltage arena that is the desirable area of operation. The target operating voltage (VDD) range was from 2.0V to 3.0V. It should be noted that the 0.5μm AMI process used in the fabrication of the chip is a 3.3V-5.0V process, and not a low voltage process. A process temperature range of 0°C to 70° was used as the temperature range of evaluation. This is the standard cell data sheet range of operation for this process.

Based on these criteria, and through simulation trial and error,  $R_{ref}$  was initially set to  $35k\Omega$  instead of the calculated  $145k\Omega$ . Simulation indicated that at  $R_{ref}$  of  $145k\Omega$ , the output voltage was closer to  $0.7V$ . This variation is mostly due to the estimate made of the diode current in the calculation (set at  $1\mu A$ ) vs. the later measured  $I_{diode}$  of approximately  $3\mu A$ . Thus a value of  $35k\Omega$  was used, with  $R_{ref}$  being refined later once the actual results could be evaluated. This  $35k\Omega$  value provided a starting point for the evaluation. The final SPICE netlist is included as attachment A.

The final circuit was simulated resulting in the simulated results shown in Figure 4.3. The starting point varies because the startup circuit used in the design varies with temperature. Because the startup circuit was considered a potential problem during the preliminary design phase, it was bonded out in the actual layout so the BGR could be evaluated independently of the startup circuit.

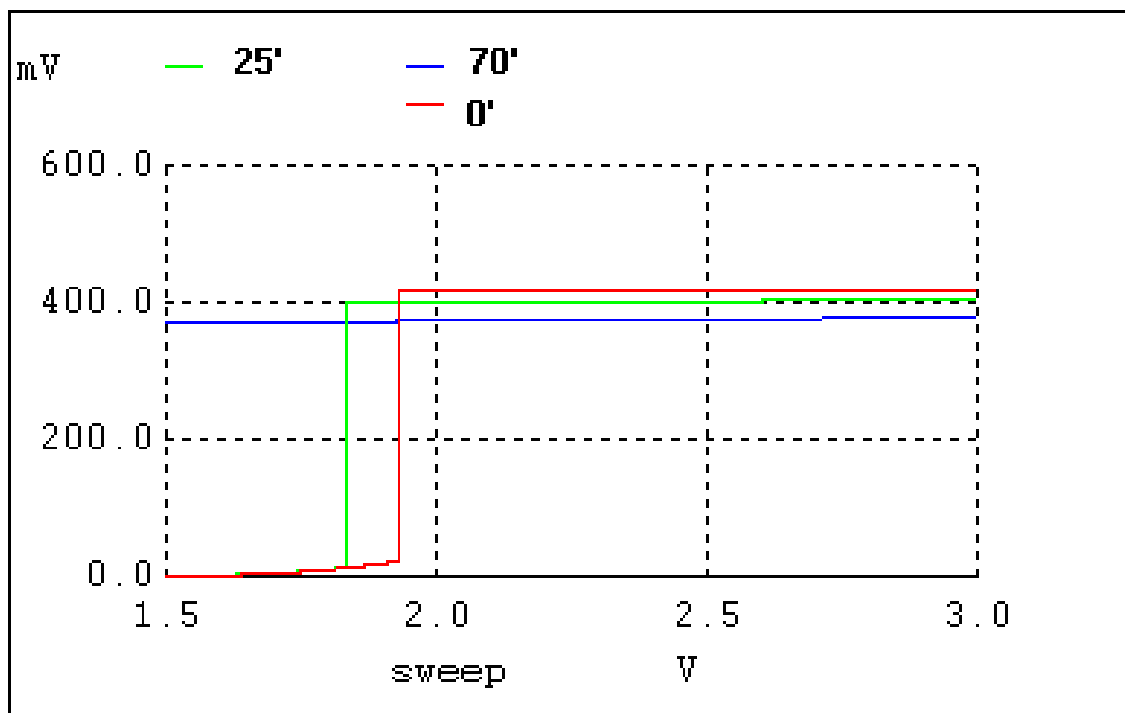


**Figure 4.3 BGR Simulation Results**

The final circuit was then built using the values for R, N and L based on these simulation results, as shown in Figure 4.4.

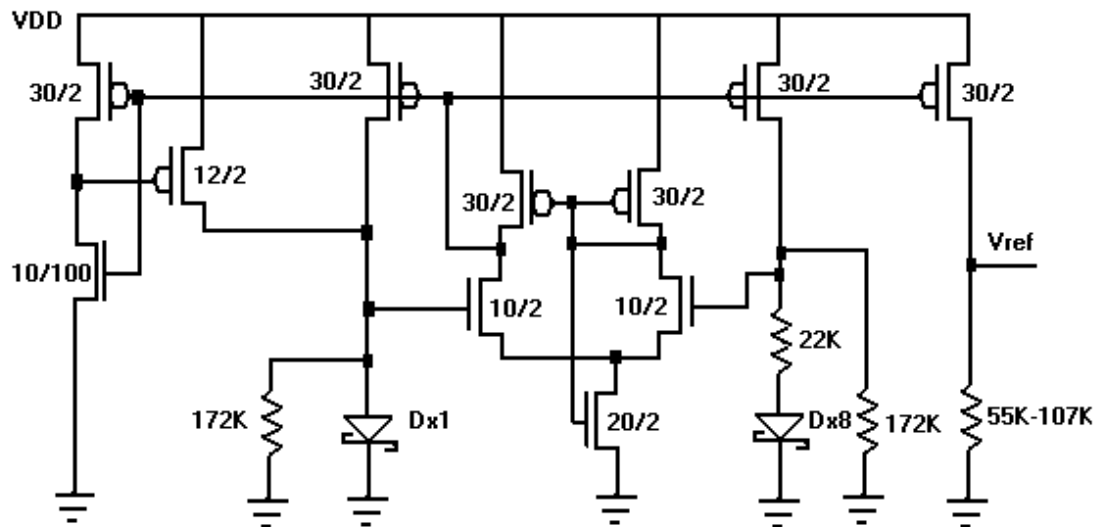


**Figure 4.4 Final BGR Design**

Note that Rref values differ from the original 35k $\Omega$ , and varies over a 53k $\Omega$  range. These values were final trimmed values.

### BGR Circuit Measurements

The first part was measured, resulting in a Vref of 0.251V. The resulting output voltage of 0.251V at a VDD of 2.5V was lower than desired. It was expected to be necessary to “trim” the output resistor (Rref) to tune the circuit. Once Rref was trimmed to 54.8k $\Omega$ , the output shown in Figure 4.5 was produced.

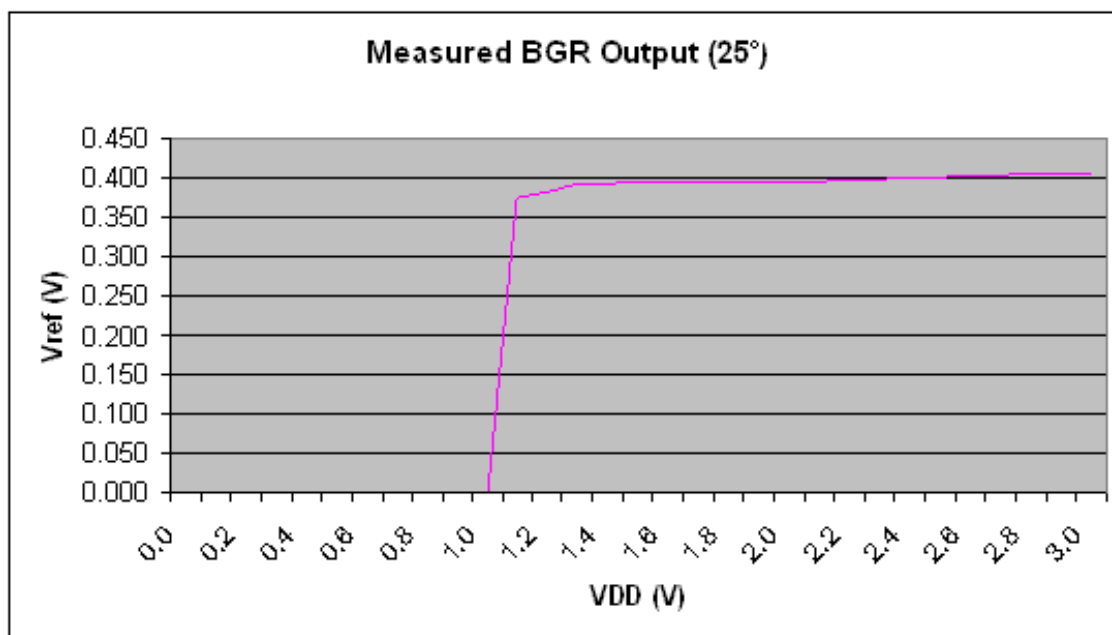


**Figure 4.5 Measured Reference Voltage**

The resulting output was relatively stable over the operating range of 2.0V to 3.0V. The startup circuit was toggled in until the circuit started (at approx 1.1V) and was then disconnected. The circuit current was approximately 23.75 $\mu$ A at 2.5V VDD and 25°C.

To examine process variation effects, all four functional parts were measured using designed initial conditions, and again after they were trimmed. (Although five parts were fabricated, only four were functional.) No failure analysis was performed on the failing circuit. The pre-post trim results can be seen in Figure 4.6.



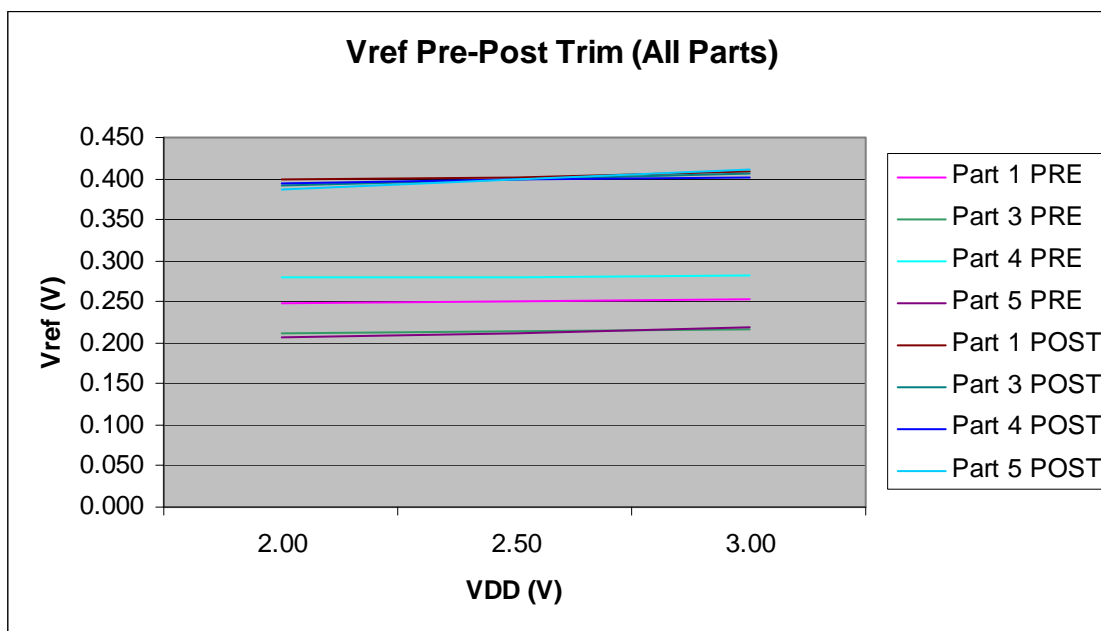


**Figure 4.6 Pre-Post Trim Measurements**

The four parts initially (as set based on the SPICE model) had a lower than simulated reference voltage, and over a range of almost 80mV. These are the four lower lines in the figure. An obvious process variation is evident. Although some measurement error is always present, it is not expected to account for such a large distribution. It should be noted that later refinement of the SPICE model and diode model brought the simulation mean closer to 0.4V at 2.5V VDD.

Once the parts were trimmed to 0.4V at 2.5V VDD, (with an external resistor  $R_{ref}$ ) the resulting reference voltages were very consistent over the operating range. These are the four upper lines displayed in Figure 4.6. They overlap and appear as almost one line. Over the operating voltage range (from 2.0V to 3.0V VDD), the reference voltage shift across the four parts were 7mV, 8mV, 14mV and 24mV.

The temperature effects were also evaluated. Figure 4.7 shows the operation of the circuit as measured at 0°C and at 70°C.

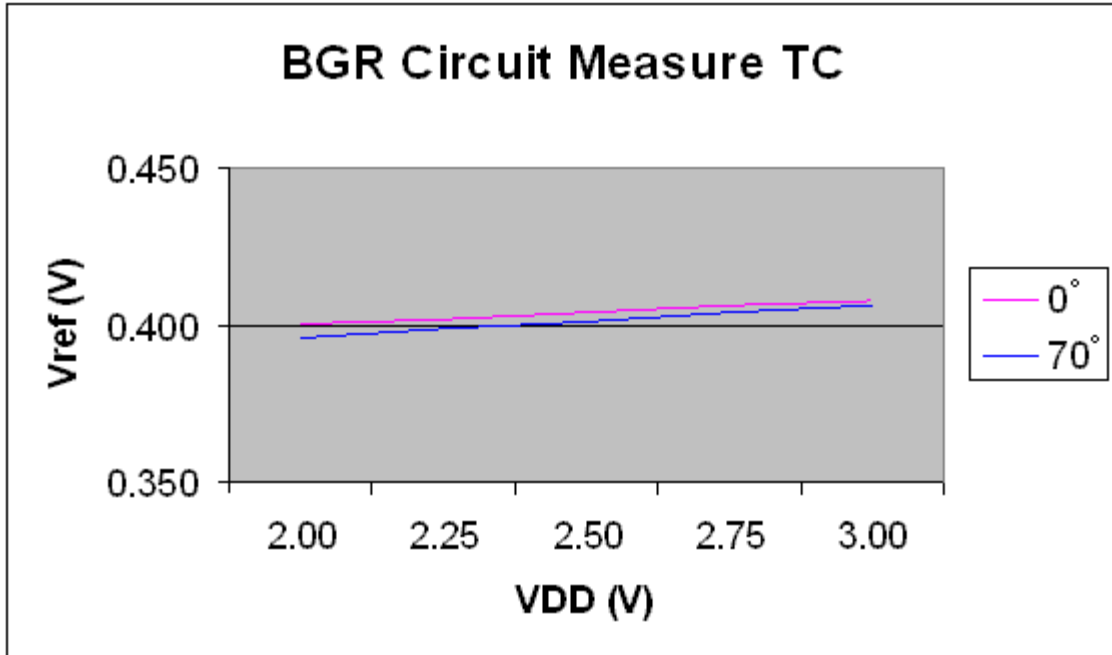


**Figure 4.7 BGR Temperature Behavior**

As is evident in Figure 4.7, there is little temperature variation between the minimum and maximum operating ranges. The TC of this part was calculated at 2.5V VDD using Equation 4.7 [8].

$$TC = \frac{1}{V_{REF}} \left( \frac{\partial V}{\partial T} \right) = \frac{1}{V_{REF}} \left( \frac{V_{REF \max} - V_{REF \min}}{T_{\max} - T_{\min}} \right) * 10^6 \quad \text{EQ 4.7}$$

$$TC = \frac{1}{0.4} \left( \frac{0.401 - 0.404}{70 - 0} \right) * 10^6 = -107 \text{ ppm/}^\circ\text{C}$$

This is better than simulation results indicated, and indicates a voltage variation of only  $43\mu\text{V}/^\circ\text{C}$ . Other parts tested were 214, 286, and  $500\text{ppm}/^\circ\text{C}$ .

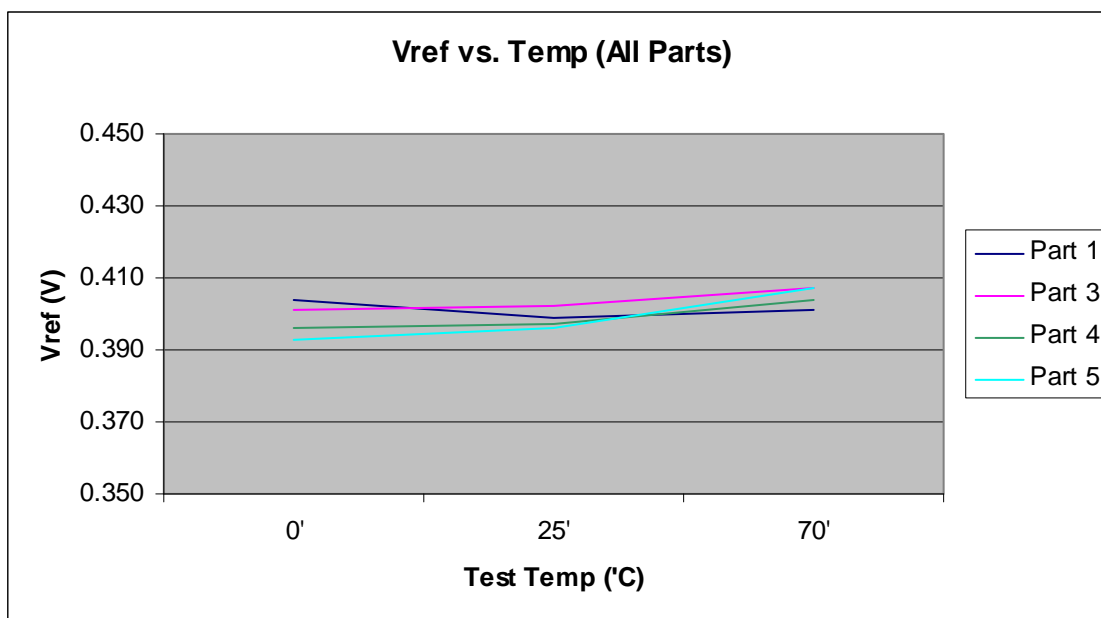


**Figure 4.8 BGR Thermal Comparison**

Again note the variation between devices. These measurements (as well as the earlier voltage measurements) were taken in the same socket using the same external components and test apparatus. The only external variation was the resistance trim applied to the Rref resistor.

As a final evaluation, the external resistor Rref on one part was trimmed to achieve a  $100\text{mV}$  Vref at  $2.5\text{V}$  VDD. Although the circuit resistor values were not optimized for this reference voltage, the BGR was evaluated simply at  $25^\circ\text{C}$  to determine if functionality was possible at this voltage by trimming alone. Resistor Rref was trimmed

at 2.5V to 23.14k $\Omega$ , where  $V_{ref}$  was at 0.10V. Over the 2.0V to 3.0V VDD range, the circuit operated well, with  $V_{ref}$  varied only 2.2mV over the 1.0V range.

### **Diode Process Variation Evaluation**

Initially only a few diodes were evaluated, to get an approximated SPICE model so the circuit could be simulated, since the BGR design is the fundamental object of this study. But to explore the reason behind the circuit variations, further testing was conducted. One BGR circuit was tested at 25°C and 2.5V VDD. It was set to a reference voltage of 400mV, then while all other factors remained the same (even the same diode set was used for DK) the diode D1 was replaced one at a time with all other single functional diodes. The  $V_{ref}$  changed considerably as the BGR was operated with the different diodes indicating that the diodes did contribute significantly to variations in the reference voltage. Reference voltages ranged from 0.185V to 0.462V with D1 as the only variable. Then all MS diodes I-V curves were measured over a 0V to 0.6V range at 25°C. The modeling of all diodes using a HP 4156 parameter analyzer produced the graph shown in Figure 4.9. Note the significant variation of the single diode (x1) distribution, and the reducing distribution on the x2, x4 and then minimal distribution of the x8 diode structures.

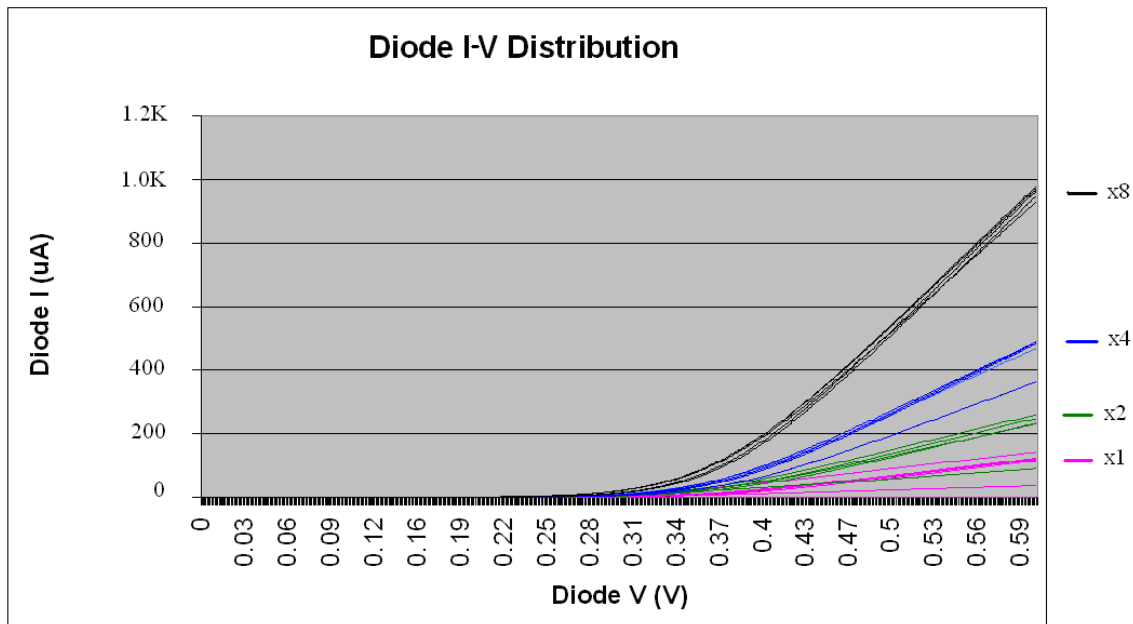


**Figure 4.9 MS Diode I-V Distribution**

Further, the diodes threshold voltages ( $V_t$ ) were compared. For the purpose of equal comparison, the diode threshold voltage was arbitrarily defined as where the diode conducted  $5\mu\text{A}$  of current. The results can be seen in Figure 4.10. Note the large distribution of the single diodes vs. the smaller distribution of the x8 diode structures. It should be noted that one single diode was excluded from this distribution as  $5\mu\text{A}$  of current was never achieved, even at 0.6V external voltage.

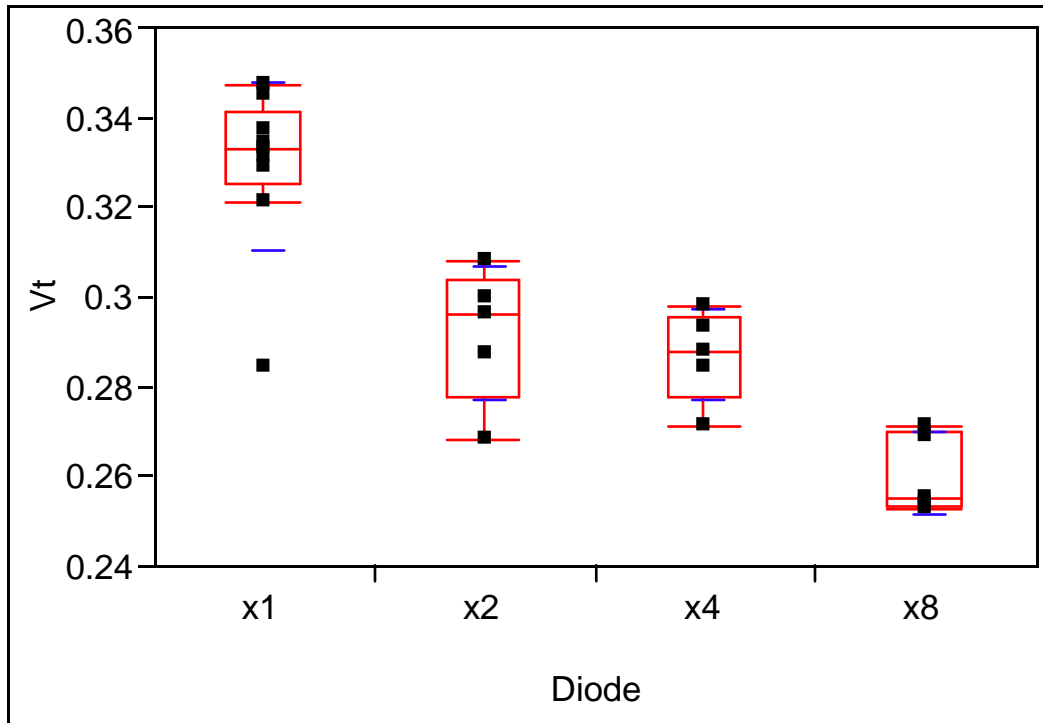


**Figure 4.10 MS Diode  $V_t$  Distribution**

The  $V_t$  point itself is lower for the multiple diode structures as is expected, since multiple diodes are connected in parallel. In addition to allowing for a tighter distribution, this attribute may also benefit the design as a lower diode  $V_t$  allows for lower reference voltage generation. Based on these results, the diode model was modified to more closely match these more quantitative results. (See appendix A.)

## CHAPTER FIVE: CONCLUSION

### **Conclusion**

The results indicate that the BGR design utilizing Schottky diodes was functional over the intended operating voltage and temperature ranges. Further, the design actually operated better than simulation results indicated, both in relation to temperature and voltage behavior. Although there was evidence of significant initial condition variation induced by process variation, the post trim results indicated this variation could be minimized.

### **Future Work**

During the course of the diode and circuit evaluation, it was discovered that there were several areas that could offer BGR improvements. The three main areas of possible improvement that were focused on are noted here.

1) Future work could be performed on the design of the same BGR circuit, but utilizing multiple MS diode structures for D1 instead of a single diode. Multiples of DK would also be utilized. Given the variations in the single diode, and the lack of variation of the multiple diode structures, it appears that using multiple structures could help minimize process variation effects and thus make the circuit operation more predictable. It would also seem likely to have the effect of reducing the probability of a single diode defect causing the circuit to fail, as an open (or high resistance) in one diode would be mitigated

by the operation of the other diodes. Another benefit would be the reduced  $V_t$  of the multiple diode structure as seen in Figure 4.10, allowing for even lower  $V_{ref}$  generation. One concern is that higher current flow may be an issue.

Since there were few diode structures available for evaluation (only six in each of the five devices), a comprehensive study of more diodes would be necessary to provide a more statistically significant indication of the process capabilities and diode variation.

2) Another area that could be further investigated is the use of the circuit shown in Figure 5.1, to generate a less temperature sensitive circuit, while generating a lower reference voltage by using Schottky diodes [10]. This circuit design was proposed to reduce the input common mode range of the added amplifier [1] [10].

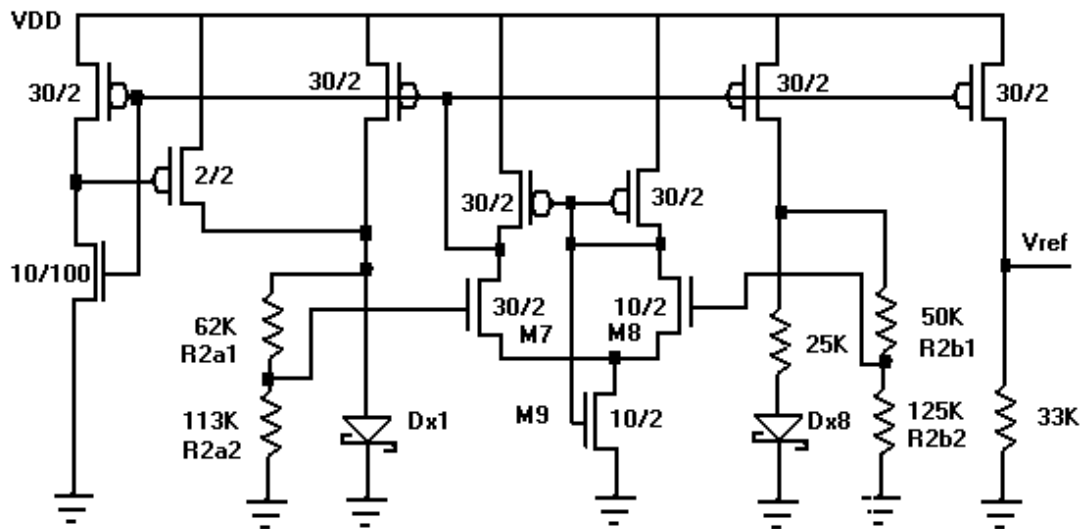


**Figure 5.1 Future BGR Design**



This circuit was not tested directly, but simulations were performed that showed the circuit would work with the modeled MS diodes. This circuit output displayed minimal thermal variation over the operating range as can be seen in Figure 5.2. It is also optimized (based again on simulation results) by increasing the width of M7 to 30 lambda, as well as increasing the resistance of R2a1 while reducing R2a2. This keeps the total resistance equal to R2, but with the effect of lowering the Vg of M7. The net simulation result is actually a thermal crossover at the point of interest (2.5V) as seen in Figure 5.2. This would indicate a temperature coefficient of 0ppm/°C at that point. This target may be further enhanced by allowing a trimming of R2a1 and R2a2 post fabrication.

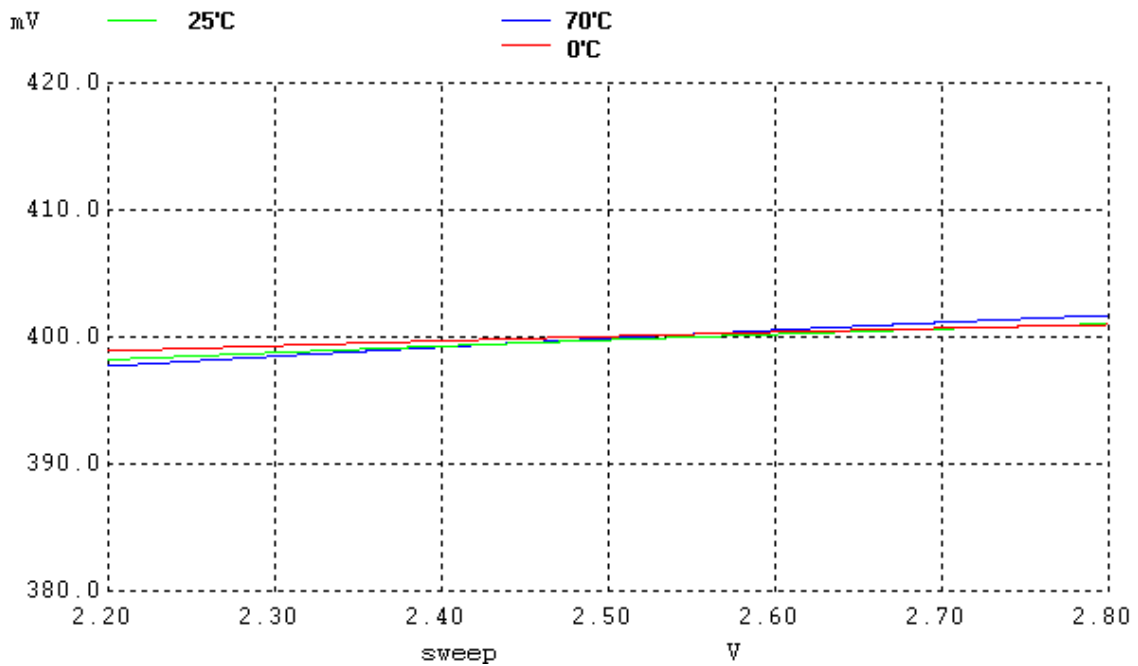


**Figure 5.2 Future BGR Simulation**

As can be seen in Equation 5.1 below, the lower MS diode voltage (replacing  $V_{EB2}$  in the equation with MS diode  $V_t$ ) would result in a lower possible reference voltage [11].

$$V_{REF} = \frac{R_{REF}}{R_2} \left( V_{EB2} + V_T \left[ \frac{R_{2A1} + R_{2A2}}{R} \right] \ln K \right) \quad \text{EQ 5.1}$$

A SPICE netlist of the simulated circuit is included in appendix B.

**3)** Another area for improvement is in the application of the startup circuit. While that component of the circuit was not the focus of the design evaluation, and therefore not aggressively pursued, it would be necessary to have a more reliable startup circuit in an actual design implementation of the BGR circuit in an application.

## REFERENCES

- 1 R. Jacob Baker, "CMOS Circuit Design, Layout and Simulation" 2<sup>nd</sup> edition  
Wiley Interscience, 2005 pp745-770
- 2 Karl Hess, "Advanced Theory of Semiconductor Devices"  
IEEE Press, 2000 pp194-201
- 3 B. Van Zeghbroeck "Metal-Semiconductor Junctions" 2004  
<[http://ece-www.colorado.edu/~bart/book/book/chapter3/ch3\\_2.htm#3\\_2\\_2](http://ece-www.colorado.edu/~bart/book/book/chapter3/ch3_2.htm#3_2_2)>
- 4 Leonard J. Brillson, "Contacts to Semiconductors, Fundamentals and  
Technology" Noyes Publications, 1993 pp176-291
- 5 Ouse Tech, WinSpice Version 1.05.07  
<<http://www.winspice.co.uk/>>
- 6 Dr. D. E. Boyce, LASI [Layout System for Individuals] Version 7.0.2.7  
<<http://members.aol.com/lasicad/>>
- 7 MOSIS "Low-Cost Prototyping and Small-Volume Production Service"  
<<http://www.mosis.org/>>
- 8 AMIS [C5N Process]  
<<http://www.mosis.org/products/fab/vendors/amis/c5/>>
- 9 Dieter K. Schroder, "Semiconductor Material and Device Characterization"  
2<sup>nd</sup> edition, Wiley Interscience, 1998 pp169-208
- 10 Ka Nang Leung & Philip K. T. Mok, "A Sub-1-V 15ppm/°C CMOS Bandgap  
Voltage Reference Without Requiring Low Threshold Voltage Device"  
IEEE Journal of Solid State Circuits, vol 37, no 4, April 2003 pp526-530
- 11 Ban P. Wong, et al., "Nano-CMOS Circuit and Physical Design"  
Wiley Interscience, 2005 pp154-155

APPENDIX A

**Final Design Netlist**

## Final Design Netlist

```
.control
destroy all
set temp=0
run
set temp=25
run
set temp=70
run
plot VDD dc1.vrf dc2.vrf dc3.vrf
plot dc1.vrf dc2.vrf dc3.vrf xlimit 1.9 3.0 ylimit 0 0.5
.endc

.option scale=0.3u
.dc VDD 0 3.0 1m

VDD VDD 0 DC 3.0V
M1 V1 Vbs VDD VDD CMOSP L=2 W=30
M2 V1 Vbs 0 0 CMOSN L=100 W=10
M3 V2 V1 VDD VDD CMOSP L=2 W=12
M4 V2 Vbs VDD VDD CMOSP L=2 W=30

M5 Vbs V4 VDD VDD CMOSP L=2 W=30
M6 V4 V4 VDD VDD CMOSP L=2 W=30
M7 Vbs V2 V3 0 CMOSN L=2 W=15
*modeled as W=15 to get circuit to start
M8 V4 V5 V3 0 CMOSN L=2 W=10
M9 V3 V4 0 0 CMOSN L=2 W=20

M10 V5 Vbs VDD VDD CMOSP L=2 W=30
M11 Vrf Vbs VDD VDD CMOSP L=2 W=30

R1 V2 0 RMODEL 172k
R2 V5 V6 RMODEL 22k
R3 V5 0 RMODEL 172k
R4 Vrf 0 RMODEL 60k

D1 V2 0 SCHOTTKY
D2 V6 0 SCHOTTKY 8

* T4BP SPICE BSIM3 VERSION 3.1 PARAMETERS
*SPICE 3f5 Level 8, Star-HSPICE Level 49, UTMOST Level 8
* DATE: Jan 31/05
* LOT: T4BP WAF: 9104
* Temperature_parameters=Default

.MODEL SCHOTTKY D IS=7e-18 N=0.43 XTI=3 RS=2.2K TC1=-0.002

.MODEL RMODEL R TC1=0.002

.MODEL CMOSN NMOS LEVEL = 8
```

+TNOM = 27 TOX = 1.42E-8  
 +XJ = 1.5E-7 NCH = 1.7E17 VTH0 = 0.5873345  
 +K1 = 0.9230324 K2 = -0.1047761 K3 = 22.4916147  
 +K3B = -9.1266087 W0 = 1E-8 NLX = 2.000399E-9  
 +DVT0W = 0 DVT1W = 0 DVT2W = 0  
 +DVT0 = 2.2994082 DVT1 = 0.4970166 DVT2 = -0.1842143  
 +U0 = 446.7488201 UA = 1E-13 UB = 1.299367E-18  
 +UC = 1.248923E-13 VSAT = 1.59167E5 A0 = 0.6101847  
 +AGS = 0.1302919 B0 = 2.533749E-6 B1 = 5E-6  
 +KETA = -1.666578E-3 A1 = 3.485566E-4 A2 = 0.3674233  
 +RDSW = 1.368085E3 PRWG = 0.0600883 PRWB = 0.0171806  
 +WR = 1 WINT = 2.09488E-7 LINT = 7.220693E-8  
 +XL = 1E-7 XW = 0 DWG = 2.605489E-9  
 +DWB = 4.277159E-8 VOFF = -0.0115079 NFACTOR = 0.7015054  
 +CIT = 0 CDSC = 2.4E-4 CDSCD = 0  
 +CDSCB = 0 ETA0 = 0.0031556 ETAB = -4.218915E-3  
 +DSUB = 0.4129659 PCLM = 2.4387548 PDIBLC1 = 1  
 +PDIBLC2 = 4.31964E-3 PDIBLCB = 0.053704 DROUT = 0.9257597  
 +PSCBE1 = 6.241157E8 PSCBE2 = 1.459532E-4 PVAG = 0  
 +DELTA = 0.01 RSH = 83.1 MOBMOD = 1  
 +PRT = 0 UTE = -1.5 KT1 = -0.11  
 +KT1L = 0 KT2 = 0.022 UA1 = 4.31E-9  
 +UB1 = -7.61E-18 UC1 = -5.6E-11 AT = 3.3E4  
 +WL = 0 WLN = 1 WW = 0  
 +WWN = 1 WWL = 0 LL = 0  
 +LLN = 1 LW = 0 LWN = 1  
 +LWL = 0 CAPMOD = 2 XPART = 0.5  
 +CGDO = 1.92E-10 CGSO = 1.92E-10 CGBO = 1E-9  
 +CJ = 4.303837E-4 PB = 0.9074906 MJ = 0.4317275  
 +CJSW = 3.001226E-10 PBSW = 0.8 MJSW = 0.1714547  
 +CJSWG = 1.64E-10 PBSWG = 0.8 MJSWG = 0.1714547  
 +CF = 0 PVTH0 = 0.0628352 PRDSW = 346.0290637  
 +PK2 = -0.0296479 WKETA = -0.0177686 LKETA = -2.260032E-3

.MODEL CMOS PMOS LEVEL = 8  
 +TNOM = 27 TOX = 1.42E-8  
 +XJ = 1.5E-7 NCH = 1.7E17 VTH0 = -0.9286607  
 +K1 = 0.5412389 K2 = 0.0128372 K3 = 11.1025735  
 +K3B = -0.8099316 W0 = 3.891267E-7 NLX = 1.278268E-8  
 +DVT0W = 0 DVT1W = 0 DVT2W = 0  
 +DVT0 = 2.2645652 DVT1 = 0.7212046 DVT2 = -0.1560945  
 +U0 = 200.0599104 UA = 2.439885E-9 UB = 1.928396E-21  
 +UC = -7.00689E-11 VSAT = 1.808499E5 A0 = 0.9334131  
 +AGS = 0.1371285 B0 = 2.423807E-7 B1 = 1.124249E-6  
 +KETA = -2.535624E-3 A1 = 9.577499E-5 A2 = 0.3  
 +RDSW = 3E3 PRWG = 0.0148859 PRWB = -0.0125106  
 +WR = 1 WINT = 2.409073E-7 LINT = 8.424942E-8  
 +XL = 1E-7 XW = 0 DWG = -1.818861E-9  
 +DWB = 2.399629E-8 VOFF = -0.0801078 NFACTOR = 0.4609732  
 +CIT = 0 CDSC = 2.4E-4 CDSCD = 0  
 +CDSCB = 0 ETA0 = 0.0372311 ETAB = -0.0981321  
 +DSUB = 1 PCLM = 2.1048606 PDIBLC1 = 0.0586727  
 +PDIBLC2 = 3.988846E-3 PDIBLCB = -0.0530319 DROUT = 0.2623986  
 +PSCBE1 = 5.313202E9 PSCBE2 = 5E-10 PVAG = 0

```
+DELTA = 0.01      RSH  = 105.2      MOBMOD = 1
+PRT   = 0         UTE  = -1.5       KT1   = -0.11
+KT1L  = 0         KT2  = 0.022      UA1   = 4.31E-9
+UB1   = -7.61E-18 UC1  = -5.6E-11    AT    = 3.3E4
+WL    = 0         WLN  = 1         WW    = 0
+WWN   = 1         WWL  = 0         LL    = 0
+LLN   = 1         LW   = 0         LWN   = 1
+LWL   = 0         CAPMOD = 2        XPART = 0.5
+CGDO  = 2.28E-10  CGSO  = 2.28E-10  CGBO  = 1E-9
+CJ    = 7.334167E-4 PB   = 0.9498634  MJ    = 0.4952447
+CJSW  = 2.898167E-10 PBSW  = 0.99      MJSW  = 0.3046906
+CJSWG = 6.4E-11   PBSWG = 0.99      MJSWG = 0.3046906
+CF    = 0         PVTH0 = 5.98016E-3  PRDSW = 14.8598424
+PK2   = 3.73981E-3 WKETA = 8.333721E-3  LKETA = -6.867545E-3

.end
```

APPENDIX B

**Future Design Netlist**



## Future Design Netlist

```
.control
destroy all
set temp=0
run
set temp=25
run
set temp=70
run
plot vdd Vrf dc1.vrf dc2.vrf dc3.vrf
plot dc1.vrf dc2.vrf dc3.vrf  xlimit 2.25 2.75 ylimit 0.38 0.42
.endc
```

```
.option scale=0.3u
.dc VDD 0 3 1m
```

```
VDD VDD 0 DC 3V
```

```
M1 V1 Vbs VDD VDD CMOS L=2 W=30
M2 V1 Vbs 0 0 CMOSN L=100 W=10
M3 V2 V1 VDD VDD CMOS L=2 W=2
M4 V2 Vbs VDD VDD CMOS L=2 W=30
```

```
M5 Vbs V4 VDD VDD CMOS L=2 W=30
M6 V4 V4 VDD VDD CMOS L=2 W=30
M7 Vbs Vn V3 0 CMOSN L=2 W=30
M8 V4 Vp V3 0 CMOSN L=2 W=10
M9 V3 V4 0 0 CMOSN L=2 W=10
```

```
M10 V5 Vbs VDD VDD CMOS L=2 W=30
M11 Vrf Vbs VDD VDD CMOS L=2 W=30
```

```
R1a V2 Vn RMODEL 62k
R1b Vn 0 RMODEL 113k
R2 V5 V6 RMODEL 25k
R3a V5 Vp RMODEL 50k
R3b Vp 0 RMODEL 125k
R4 Vrf 0 RMODEL 33.6k
```

```
D1 V2 0 SCHOTTKY
D2 V6 0 SCHOTTKY 8
```

```
* T4BP SPICE BSIM3 VERSION 3.1 PARAMETERS
*SPICE 3f5 Level 8, Star-HSPICE Level 49, UTMOST Level 8
* DATE: Jan 31/05
* LOT: T4BP WAF: 9104
* Temperature_parameters=Default
```

```
.MODEL SCHOTTKY D IS=4e-18 N=0.41 XTI=3 RS=3.3K
```

```
.MODEL RMODEL R TC1=0.002
```

```

.MODEL CMOSN NMOS LEVEL = 8
+TNOM = 27      TOX = 1.42E-8
+XJ  = 1.5E-7   NCH = 1.7E17   VTH0 = 0.5873345
+K1  = 0.9230324 K2 = -0.1047761 K3 = 22.4916147
+K3B = -9.1266087 W0 = 1E-8     NLX = 2.000399E-9
+DVT0W = 0      DVT1W = 0      DVT2W = 0
+DVT0 = 2.2994082 DVT1 = 0.4970166 DVT2 = -0.1842143
+U0  = 446.7488201 UA = 1E-13   UB = 1.299367E-18
+UC  = 1.248923E-13 VSAT = 1.59167E5 A0 = 0.6101847
+AGS = 0.1302919 B0 = 2.533749E-6 B1 = 5E-6
+KETA = -1.666578E-3 A1 = 3.485566E-4 A2 = 0.3674233
+RDSW = 1.368085E3 PRWG = 0.0600883 PRWB = 0.0171806
+WR  = 1        WINT = 2.09488E-7 LINT = 7.220693E-8
+XL  = 1E-7     XW  = 0         DWG = 2.605489E-9
+DWB = 4.277159E-8 VOFF = -0.0115079 NFACTOR = 0.7015054
+CIT = 0        CDSC = 2.4E-4   CDSCD = 0
+CDSCB = 0      ETA0 = 0.0031556 ETAB = -4.218915E-3
+DSUB = 0.4129659 PCLM = 2.4387548 PDIBLC1 = 1
+PDIBLC2 = 4.31964E-3 PDIBLCB = 0.053704 DROUT = 0.9257597
+PSCBE1 = 6.241157E8 PSCBE2 = 1.459532E-4 PVAG = 0
+DELTA = 0.01   RSH = 83.1     MOBMOD = 1
+PRT = 0        UTE = -1.5     KT1 = -0.11
+KTIL = 0       KT2 = 0.022   UA1 = 4.31E-9
+UB1 = -7.61E-18 UC1 = -5.6E-11 AT = 3.3E4
+WL  = 0        WLN = 1       WW  = 0
+WWN = 1        WWL = 0       LL  = 0
+LLN = 1        LW  = 0       LWN = 1
+LWL = 0        CAPMOD = 2     XPART = 0.5
+CGDO = 1.92E-10 CGSO = 1.92E-10 CGBO = 1E-9
+CJ  = 4.303837E-4 PB = 0.9074906 MJ = 0.4317275
+CJSW = 3.001226E-10 PBSW = 0.8 MJSW = 0.1714547
+CJSWG = 1.64E-10 PBSWG = 0.8 MJSWG = 0.1714547
+CF  = 0        PVTH0 = 0.0628352 PRDSW = 346.0290637
+PK2 = -0.0296479 WKETA = -0.0177686 LKETA = -2.260032E-3

```

```

.MODEL CMOSP PMOS LEVEL = 8
+TNOM = 27      TOX = 1.42E-8
+XJ  = 1.5E-7   NCH = 1.7E17   VTH0 = -0.9286607
+K1  = 0.5412389 K2 = 0.0128372 K3 = 11.1025735
+K3B = -0.8099316 W0 = 3.891267E-7 NLX = 1.278268E-8
+DVT0W = 0      DVT1W = 0      DVT2W = 0
+DVT0 = 2.2645652 DVT1 = 0.7212046 DVT2 = -0.1560945
+U0  = 200.0599104 UA = 2.439885E-9 UB = 1.928396E-21
+UC  = -7.00689E-11 VSAT = 1.808499E5 A0 = 0.9334131
+AGS = 0.1371285 B0 = 2.423807E-7 B1 = 1.124249E-6
+KETA = -2.535624E-3 A1 = 9.577499E-5 A2 = 0.3
+RDSW = 3E3     PRWG = 0.0148859 PRWB = -0.0125106
+WR  = 1        WINT = 2.409073E-7 LINT = 8.424942E-8
+XL  = 1E-7     XW  = 0         DWG = -1.818861E-9
+DWB = 2.399629E-8 VOFF = -0.0801078 NFACTOR = 0.4609732
+CIT = 0        CDSC = 2.4E-4   CDSCD = 0
+CDSCB = 0      ETA0 = 0.0372311 ETAB = -0.0981321
+DSUB = 1       PCLM = 2.1048606 PDIBLC1 = 0.0586727

```

+PDIBLC2 = 3.988846E-3 PDIBLCB = -0.0530319 DROUT = 0.2623986  
+PSCBE1 = 5.313202E9 PSCBE2 = 5E-10 PVAG = 0  
+DELTA = 0.01 RSH = 105.2 MOBMOD = 1  
+PRT = 0 UTE = -1.5 KT1 = -0.11  
+KT1L = 0 KT2 = 0.022 UA1 = 4.31E-9  
+UB1 = -7.61E-18 UC1 = -5.6E-11 AT = 3.3E4  
+WL = 0 WLN = 1 WW = 0  
+WWN = 1 WWL = 0 LL = 0  
+LLN = 1 LW = 0 LWN = 1  
+LWL = 0 CAPMOD = 2 XPART = 0.5  
+CGDO = 2.28E-10 CGSO = 2.28E-10 CGBO = 1E-9  
+CJ = 7.334167E-4 PB = 0.9498634 MJ = 0.4952447  
+CJSW = 2.898167E-10 PBSW = 0.99 MJSW = 0.3046906  
+CJSWG = 6.4E-11 PBSWG = 0.99 MJSWG = 0.3046906  
+CF = 0 PVTH0 = 5.98016E-3 PRDSW = 14.8598424  
+PK2 = 3.73981E-3 WKETA = 8.333721E-3 LKETA = -6.867545E-3

.end